

RobotMover: Learning to Move Large Objects by Imitating the Dynamic Chain

Tianyu Li^{1,*}, Joanne Truong², Jimmy Yang², Alexander Clegg², Akshara Rai², Sehoon Ha¹, Xavier Puig²

¹Georgia Institute of Technology, ²FAIR, Meta

*Work done during an internship at FAIR, Meta.

Email: tli471@gatech.edu



Fig. 1: RobotMover enables robots to move a variety of large objects.

Abstract—Moving large objects, such as furniture, is a critical capability for robots operating in human environments. This task presents significant challenges due to two key factors: the need to synchronize whole-body movements to prevent collisions between the robot and the object, and the under-actuated dynamics arising from the substantial size and weight of the objects. These challenges also complicate performing these tasks via teleoperation. In this work, we introduce RobotMover, a generalizable learning framework that leverages human-object interaction demonstrations to enable robots to perform large object manipulation tasks. Central to our approach is the Dynamic Chain, a novel representation that abstracts human-object interactions so that they can be retargeted to robotic morphologies. The Dynamic Chain is a spatial descriptor connecting the human and object root position via a chain of nodes, which encode the position and velocity of different interaction keypoints. We train policies in simulation using Dynamic-Chain-based imitation rewards and domain randomization, enabling zero-shot transfer to real-world settings without fine-tuning. Our approach outperforms both learning-based methods and teleoperation baselines across six evaluation metrics when tested on three distinct object types, both in simulation and on physical hardware. Furthermore, we successfully apply the learned policies to real-world tasks, such as moving a trash cart and rearranging chairs.

I. INTRODUCTION

Moving large objects such as furniture is a common challenge in human spaces. Whether it is rearranging a living room or organizing a workspace, these tasks often require significant effort. While people have traditionally handled these tasks independently, there is an increasing interest in developing autonomous robots that can help. The ability for robots to assist in moving large objects would not only reduce physical strain on humans, but also enable greater efficiency in various settings, ranging from households to industrial logistics.

While there has been significant progress in enabling robots to rearrange small items [1, 6, 4, 34], manipulating large objects presents a unique set of challenges. These challenges arise in two areas, as illustrated in Figure 2. First, when objects are large enough, they impose non-negligible spatial constraints. Without advanced control policies, the object may collide with the robot or its surroundings, potentially causing damage to both the system and the object. Second, large objects typically exceed the lifting capacity of most robots, requiring robots to manage the object’s momentum

and overcome the ground friction during movement. These challenges require developing dynamic control policies that can synchronize the movements of the manipulator and the object, and address the under-actuated nature of large object manipulation tasks.

Several approaches have been proposed to address these challenges. Model-based methods rely on accurately modeling the dynamics of the robot, the object, and their interactions. However, modeling a wide range of object interactions and dynamics is challenging, limiting the generalizability of these methods across different scenarios. Reinforcement learning allows robots to learn through trial and error, but requires designing reward functions that can generalize effectively across diverse objects. While imitation learning through teleoperation has shown success in various applications [25, 10, 22], this approach is limited by its reliance on skilled operators and the significant time required to collect demonstration data, particularly when manipulating large and heavy objects. These limitations highlight the need for more efficient and scalable solutions to enable robots to handle large objects effectively.

In this work, we propose RobotMover, a generalizable learning framework for robots to manipulate large objects by leveraging demonstrations of humans interacting with objects. Our framework uses human and object movements as a reference to generate an imitation reward. Using this reward, we train a control policy in a simulation environment with domain randomization, enabling zero-shot transfer to the real world. A key aspect of this approach is to overcome the morphological differences between humans and robots, which makes it infeasible to directly copy the joint angles for imitation. To resolve this, we introduce the Dynamic Chain, a novel representation for describing human-object interactions. The Dynamic Chain is a chain structure connecting every joint from the human’s root to the object’s root, with each joint serving as a vertex on the chain. The movement of the Dynamic Chain captures how humans transmit force from their “core” into the object. Compared to whole-body movements, the Dynamic Chain provides an abstract representation that can be easily retargeted to the robot’s morphology. We use the Dynamic Chain as the imitation reference to train the robot’s policy, enabling it to effectively manipulate large objects.

To evaluate the effectiveness of our method, we conduct a series of experiments in both simulated and real-world environments. In simulation, we test the Dynamic Chain framework against reinforcement learning, end-effector tracking, and inverse kinematics (IK) methods. Our results indicate that the Dynamic Chain outperforms these baselines tracking target object trajectories. On hardware, we deploy policies trained using the Dynamic Chain on a Spot robot and compare them against two learning-based baselines and two types of teleoperation. We propose six metrics to evaluate the robot’s behavior in terms of robustness, capability, and controllability. RobotMover outperforms baselines in all aspects, showcasing its adaptability and effectiveness in handling diverse large objects. Finally, by combining our learned policy with a motion planner, we demonstrate our framework in two real-world

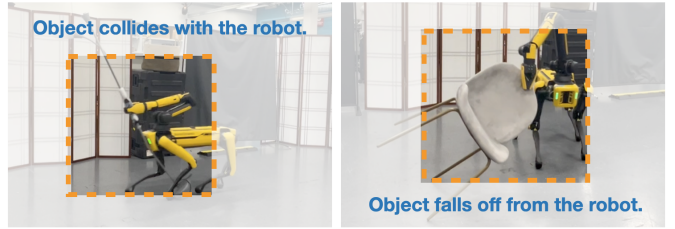


Fig. 2: Challenges of moving large objects include but not limit to object colliding with the robot and object falls off from the robot’s gripper due to high momentum.

applications: trash cart transportation and chair rearrangement, highlighting the practical utility of our approach.

In summary, this paper makes three main contributions:

- A new robot task: We propose an important and challenging robot task: *large object manipulation*, with challenges not typically encountered when manipulating small objects, such as synchronizing the robot’s whole-body movement and learning a dynamical control strategy to overcome the shape and momentum of the target objects.
- A generalizable learning framework: We introduce a generalizable learning framework for robots to manipulate large objects by imitating the Dynamic Chain derived from human-object interaction demonstrations.
- We conduct several experiments to evaluate our approach in simulation and hardware, demonstrating that our framework enables robots to reliably move diverse objects and can be used for real-world applications.

II. RELATED WORKS

A. Mobile Manipulation

Mobile manipulation tasks that involve robot locomotion and interaction capabilities have been a prominent topic in robotics research [10, 35, 40, 32, 28, 24, 9, 5, 1]. Many mobile manipulation approaches rely on model-based control, which generally requires domain expertise to design a model tailored to a system and task [17, 36, 16, 11]. Recently, learning-based approaches have been applied to mobile manipulation, alleviating much of the heavy engineering effort. These methods have addressed a variety of challenging real-world tasks, such as mobile pick-and-place [40, 33, 39, 12], manipulation of articulated objects [37, 31, 38], and long-horizon cooking tasks [10]. There has also been an interest in creating more interactive and user-friendly robotic systems by integrating primitive mobile manipulation skills with Large Language Models [35, 5, 1]. However, most prior work has focused on robots interacting with objects that are small and light, where the dynamic effects of these objects are usually negligible for manipulation. In this work, we study robot learning for rearranging large and heavy objects, such as furniture or a trash truck, where it is necessary to account for these effects.

B. Large Object Manipulation

While robots that can manipulate large objects are common in industrial applications, they operate in controlled environments, where the objects are known and the dynamics

more easily predictable. More recently, some efforts have been made to allow robots to move large objects in more uncontrolled environments, either by training them to imitate teleoperation demonstrations [10] or via curiosity-driven methods [23]. However, collecting teleoperation data is known to be time-consuming, and the collected data can only be used on the same robot platform. Curiosity-driven methods are challenging to control for real-world applications. Ravan et al. [26] addresses the problem of manipulating a wheeled chair without simulation. In this work, we introduce a generalizable learning framework that enables robots to manipulate large objects from human demonstrations.

C. Imitation Learning for Robotics

Imitation learning approaches aim to train robot policies by leveraging expert demonstrations. A common method is behavioral cloning, which learns a policy by mimicking the demonstration’s actions and has shown promising results in a wide range of robot tasks [10, 6, 15, 19, 30]. For more dynamic tasks, such as agile locomotion, demonstrations provide reference poses that be used as an imitation reward [25, 3] or an adversarial reward [8] to train policies in simulation through reinforcement learning. However, to use demonstrations as reference pose targets, the demonstrations must have the same morphology as the robot.

In settings where robots have significantly different embodiments compared to the demonstrator, such as in legged manipulators, the correspondence between the demonstrator and the robot must be properly established to transfer knowledge. This can be achieved through unsupervised learning [20, 21] or data augmentation [13]. Our work is closely related to [41], which introduces Interaction Graph as a representation for training object interactions in humanoid robots using human demonstrations. However, the Interaction Graph is a high-dimensional representation that only works between similar morphologies. In our work, we propose the Dynamic Chain, a representation that leverages human whole-body motion data to train policies for robots with different morphologies.

III. PRELIMINARY: IMITATION LEARNING

Our robot learning framework is built upon the imitation learning paradigm, which enables robots to acquire skills by learning from demonstration data. The goal is to teach the robot how to move large objects by replicating human-object interaction behaviors. We start with a demonstration trajectory $\xi = \{p_1^{ho}, p_2^{ho}, \dots, p_T^{ho}\}$, where each aggregated pose $p_t^{ho} = (p_t^h, p_t^o)$ represents the human pose p_t^h and the object pose p_t^o at time step t . These trajectories, typically acquired from motion capture systems or online datasets, form the basis for defining a reward signal that evaluates how well the robot can replicate the demonstrated behavior.

The imitation learning process is formulated as a reinforcement learning (RL) problem, where the robot learns a policy

$\pi(a_t|s_t)$ to maximize the expected cumulative reward:

$$J(\pi) = \mathbb{E} \left[\sum_{t=1}^T r(s_t, a_t) \right], \quad (1)$$

where $r(s_t, a_t) = r_t^{imi} + r_t^{reg}$ is the reward at time t , consisting of an imitation reward r_t^{imi} and a regularization reward r_t^{reg} . The imitation reward evaluates how closely the robot’s actions align with the demonstrated behaviors, while the regularization reward encourages smooth and efficient actions.

In many scenarios, the demonstrator and the robot share similar morphologies, which allows for straightforward imitation reward designs, such as directly matching poses or velocities. However, in our case, the human demonstrator and the robot have significantly different morphologies, making it challenging to apply such simple imitation reward schemes.

IV. ROBOTMOVER WITH THE DYNAMIC CHAIN

We propose RobotMover, a learning framework designed to enable robots to learn how to move large objects by imitating human-object interaction demonstrations. An overview of the framework is presented in Fig: 3. This framework addresses the challenge of embodiment differences between humans and robots by introducing a shared representation, the Dynamic Chain, which captures the core dynamics of human-object interaction. By leveraging this representation, RobotMover enables to train robust policies in simulation which can be deployed zero-shot in the real world. In this section, we first formulate the cross-embodiment imitation learning problem and outline the challenges it presents. Next, we introduce the Dynamic Chain and describe how it is used to design an imitation reward that guides the robot’s learning. Finally, we present the model representation in our framework.

A. Cross-embodiment Imitation

While imitation learning is effective for transferring skills, the dynamic and morphological differences between humans and robots pose significant challenges. These differences, such as variations in degrees of freedom and body structure, prevent direct replication of human movements. To address this, we utilize *cross-embodiment imitation learning*, which leverages a shared representation to align the interaction dynamics between human and robot.

The imitation reward function is designed to measure the alignment between the human and robot interaction dynamics:

$$r_t^{imi} \propto -\|\Psi^{ho}(p_t^{ho}) - \Psi^{ro}(p_t^{ro})\|, \quad (2)$$

where Ψ^{ho} and Ψ^{ro} are projection functions that map the human aggregated pose p_t^{ho} and robot aggregated pose $p_t^{ro} = (p_t^r, p_t^o)$ into a shared representation space. This shared representation bridges the embodiment gap, enabling the robot to evaluate and imitate human-object interactions effectively.

A critical component of cross-embodiment imitation learning is the design of appropriate shared representations and projection functions. The representation must be concise enough to be reconstructed from both robot and human poses,

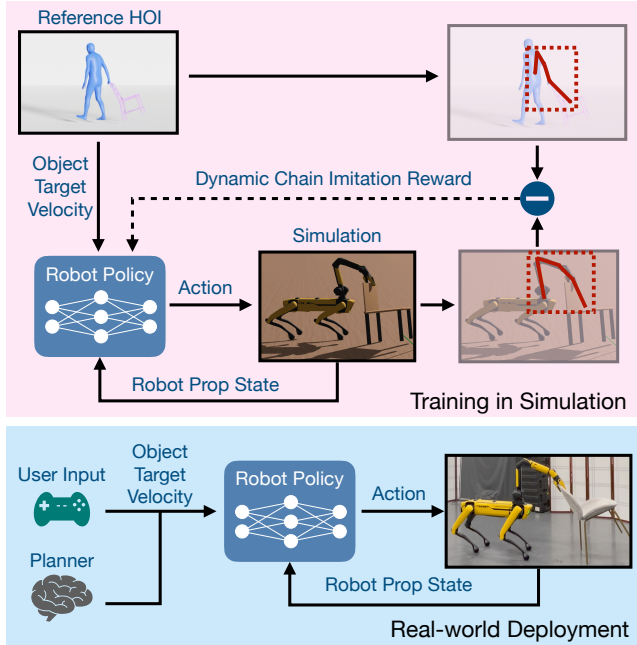


Fig. 3: Method Overview. RobotMover enables robots to learn to move large objects by imitating human-object interaction demonstrations. The framework leverages a novel representation, the Dynamic Chain, which captures the interaction dynamics between the agent and object while remaining agnostic to the agent’s embodiment. This representation is used to design an imitation reward that guides the robot’s imitation learning process.

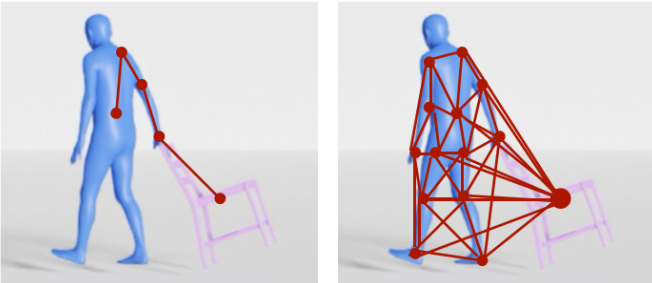


Fig. 4: Dynamic Chain (left) vs. Interaction Graph (right). The Dynamic Chain offers a simpler representation to describe agent-object interactions, which can better transfer to other morphologies. This allows us to use a human demonstration to guide the reward of a robot policy.

while also being expressive enough to capture the gist of the behavior.

B. Dynamic Chain

To effectively capture the semantics of the interaction between an agent and an object while providing a meaningful metric to guide the robot’s learning process, inspired by prior works such as Interaction Graph [41] and spatial descriptors [14], we propose the Dynamic Chain (DC), a chain-based spatial descriptor encoding the interaction information

in a sequence of nodes connected by edges. To construct the Dynamic Chain, we begin by placing a set of markers on salient locations of both the agent and the object. One end of the chain is anchored at the object’s root, while the other end is anchored at the agent’s root. Additional markers are placed at key points such as the shoulder, elbow, and the contact point between the agent and the object. The state of the agent-object dynamic chain of the is defined as $c_t^{ao} = (x_t^{ao}, q_t^{ao,i})$ where x_t^{ao} represents the object position, orientation and velocity in the global coordinate and $q_t^{ao,i}$ is the i -th dynamic chain’s orientation in the object-plane coordinate. This arrangement captures the movement of the dynamic chain and how forces are transmitted from the agent’s core to the object to trigger the object’s movement.

Figure 4 shows an example of the Dynamic Chain, with edges and nodes connecting the agent’s root to the agent’s contact point with the object’s root. The edges within the agent represent the agent’s body and arm pose, while the edge connecting the agent-object contact to the object root shows the pose of the object. The Dynamic Chain encodes both the absolute pose of the agent and objects as well as the relative positioning and dynamic coordination between these two.

Compared to Interaction Graphs [41], the Dynamic Chain is a lower-dimensional representation that focuses on capturing the essential dynamics of agent-object interaction. Interaction Graphs, by contrast, include exhaustive connections, such as edges linking a foot to the object, which can result in overly complex and unnecessary representations. This high-dimensional structure introduces challenges when transferring skills to new domains, where simplicity and interpretability are crucial. The Dynamic Chain addresses this limitation by providing a compact, low-dimensional representation that is more adaptable for skill learning and generalization.

C. Reward Design

The core of our reward design is based on the similarity between the dynamic chain of the human demonstration $c^{ho} = \Psi_{dc}^{ho}(p_t^{ho})$ and the robot’s dynamic chain during object manipulation $c^{ro} = \Psi_{dc}^{ro}(p_t^{ro})$. The imitation reward is derived by measuring the distance between the two chains, which is computed as the sum of the distances between the global positions of each corresponding node on the normalized chains:

$$err_t^c = \|x_t^{ho} - x_t^{ro}\| + \sum_{i=0}^{N-1} \alpha^i \|q_t^{ho,i} - q_t^{ro,i}\|, \quad (3)$$

Here, $\|x_t^{ho} - x_t^{ro}\|$ denote the difference between the referenced object movement and object movement triggered by the robot. α^i represents a weighting factor of the corresponding edge. We assign higher importance to edge closer to the object to emphasize precise tracking of critical points.

However, simply applying the dynamic chain difference for imitation reward calculation can lead to robot’s learning a policy which its end-effector frequently detaches from object during manipulation. This can potentially make the learned policy unstable and hard to be transferred to real world robot.

Therefore, we only give imitation reward when robot’s end-effector contacts the object. The combined imitation reward is then expressed as:

$$r_t^{imi} = e^{-err_t^c} * \mathbf{1}(f^{ee} > 0), \quad (4)$$

To enhance the overall motion quality, we include height and torque regularization, body rotation and action rate penalties from Rudin et al. [27], which encourage smoother and more efficient robot movements. These terms mitigate abrupt actions and improve the robustness of the learned policy, resulting in more natural and reliable object manipulation.

V. MODEL REPRESENTATION

The robot policy’s observation space consists of two components: the object’s target velocity and the robot’s proprioceptive data. The object’s target velocity comes from human demonstrations during training and can be given by a human or generated by a high-level planner during test time. The proprioceptive data are acquired from the robot’s onboard sensing system. The observation space excludes the object state information, such as the object’s orientation and velocity, as well as the object’s shape or visual input from the robot’s camera. This facilitates sim-to-real transfer, improves generalization across object variations, and allows us to deploy a policy without needing to provide object information. Separate policies are trained for different categories of objects to accommodate their unique dynamics. The observation space of the policy is the following:

- The object’s target velocity. (3 dims)
- The robot’s root linear and angular velocities. (6 dims)
- The robot’s joint angles. (18 dims)
- The robot’s joint velocities. (18 dims)
- The robot’s gripper open angle. (1 dim)
- The robot’s gripper contact with the object. (1 dim)

Here, the object’s target velocity is measured in the current object-plane frame. The robot’s root velocities are in the robot-plane coordinate. We test our framework in two types of simulated environments, a simple-dynamic (SD) and a full-dynamic (FD) environment, which require two different policy action spaces. The difference between these two environments will be explained in Sec: V-A. The two types of action space are:

- SD: the robot’s root velocities and arm joint angles. (13 dims)
- FD: the robot’s arm and leg joint angles. (19 dims)

To train the critic network, besides the components in the policy’s observation space, it also includes:

- The object’s target orientation in the global frame. (4 dims)
- The object’s orientation in the global frame. (4 dims)
- The object’s root linear and angular velocities. (6 dims)

Both the policy and the critic are implemented as fully connected neural networks with three hidden layers, consisting of [512, 256, 128] units, respectively, using ELU activation functions [7].

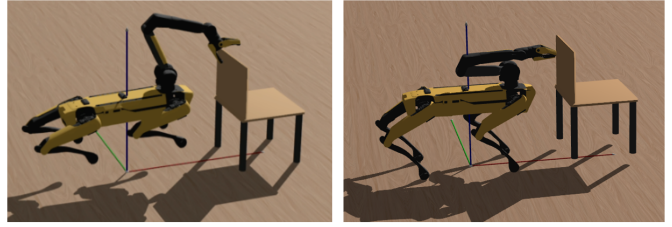


Fig. 5: Two simulation settings. Left: simple dynamic environment, without legged control. Right: fully dynamic environment, controlling all the robot’s motors.

A. Simulation Experiments Setup

VI. EXPERIMENTS

We evaluate RobotMover through experiments conducted both in simulation and on the real world. In this section, we first provide an overview of our system set. Next, we elaborate on the simulation experiment setup and present the results of the simulation experiments. We then evaluate the learned policy on hardware by comparing its performance to various baselines, including both learning-based methods and a teleoperation based method. Finally, we demonstrate the applicability of the learned object-moving policy to real-world scenarios. Our results can be best watched in the supplementary video.

A. System Setup

In our experiment, we use the Boston Dynamics Spot robot, a quadrupedal robot equipped with a robotic arm mounted on its body as our platform. It features three actuators per leg and a seven-degree-of-freedom robotic arm, including a gripper motor, resulting in a total of 19 motors. The robot’s default height is 610 mm and the robot arm’s extension up to 984 mm, the size of robot allows it to manipulate large objects. The objects involved in our experiments span a variety of shapes, including chairs, tables, and standing-stick. We train separate policies to handle each object type. The robot control policy operates at 20 Hz and is trained in Genesis simulator [2] using Proximal Policy Optimization (PPO) [29]. During training, 4096 environments are simulated in parallel on a single NVIDIA GeForce RTX 3080 Ti GPU for a period of about 4 hours. On hardware, we use the simulation trained policy without further fine-tuning.

For demonstration dataset, we utilize the OMOMO dataset [18], a high-quality motion capture dataset of human-object interactions that provides precise motion data for both humans and objects. The dataset contains all types of object involve in our experiment. During dataset collection for training a policy for a specific object, we aggregate all relevant demonstrations. For example, when training a policy for moving chairs, we include demonstrations of humans moving both wooden chairs and white chairs from the OMOMO dataset. The result demonstration collections contain diverse motion trajectories of humans moving a type of object. To simplify

motion retargeting, we exclude demonstrations involving two-arm object manipulation. However, we provide a brief analysis of using two-arm demonstrations for policy learning in Sec. VI-F. The detailed information of the dataset is provided in the appendix.

We conducted our simulation experiment on two types of simulation environments: a simplified dynamics environment and a full dynamics environment. The simplified dynamics environment is designed to align with the hardware interface, where we do not have direct control over Spot’s leg motors. In this setup, the robot policy outputs the robot’s root linear and angular velocities in the robot’s local coordinate frame, along with the desired arm poses. This results in an action space of 13 dimensions (6 for root velocities and 7 for arm poses). At each environment step, the robot’s root velocity is set to the policy output, and the physics simulation proceeds with the desired arm pose as a target. The full dynamics environment, on the other hand, is used to validate our method without the limitations imposed by the hardware interface. In this setup, the policy has access to all motor controls, leading to an action space of 19 dimensions, with each dimension corresponding to the desired pose of an individual motor.

For the objects in the simulation, we construct custom object models using primitive geometries to approximate the object models provided in the OMOMO dataset. This approach ensures that the final object shapes are similar to those in the dataset while significantly improving computational efficiency. Using the original mesh files from OMOMO, which contain complex triangular faces, would increase computational complexity during object-robot interactions, especially under contact dynamics.

When resetting the simulation environment, the robot’s xy-position is set to the origin of the simulation, and the object is placed at a position and orientation that align with the reference demonstrations. To introduce variability, we apply randomization to the robot’s initial height, as well as to the object’s initial position and orientation, its weight, and its friction coefficient. We use a single geometric model for each object type, meaning that the target object’s shape is not randomized. This decision is motivated by two key reasons. First, in our simulation setup, all objects must be loaded at the start of the simulation. During each simulation step, the contact state of every object is computed, even if only one object is manipulated in a given episode. This approach would result in significant computational overhead and slow down the simulation. Second, we argue that geometric differences in the objects are ultimately reflected in dynamic variations once the robot has grasped the object. These dynamic differences can be adequately addressed by randomizing other properties, such as friction coefficients and the object’s initial position, which effectively cover the variations caused by shape differences.

We evaluate our method by comparing it against several baseline methods. The methods used in our simulation experiments are as follows:

- **RL**: This baseline uses reinforcement learning to train a robot control policy for manipulating the target object.

The reward function is defined based on the difference between the object’s root 2D position and its reference trajectory.

- **RL-EE**: This baseline incorporates the demonstrator’s end-effector position in the global frame alongside the object’s root trajectory as imitation goals. Compared to RL, RL-EE uses the end-effector position as a heuristic to guide the exploration of the solution space, aiding policy convergence.
- **RL-IK**: Similar to RL-EE, this baseline incorporates the demonstrator’s end-effector position but in the robot’s local frame. This provides localized guidance during policy training by referencing both the object’s root trajectory and the end-effector’s position relative to the robot.
- **RobotMover (ours)**: RobotMover leverages both the object’s movement trajectory and the demonstrator’s body movement as heuristics for policy learning. This approach provides rich information for the robot, enabling it to learn skills for stable object manipulation.

These methods are evaluated based on their ability to track reference object trajectories. The tracking score v^{track} is defined as

$$v^{track} = \frac{1}{T} \sum_{t=0}^T e^{-\|x_t^{ho,xy} - x_t^{ro,xy}\|}. \quad (5)$$

here, $x_t^{ho,2d}$ and $x_t^{ro,2d}$ are referenced and experiment object xy-position, heading direction at time instance t and T represent the total time of a single experiment. The closer the object’s trajectory is to the reference, the higher the score. We run each method with 5 random seeds, and the evaluation is performed using 10 randomly sampled reference trajectories for each seed.

B. Simulation Comparison Results

Figure 6 presents a quantitative evaluation of the simulation results. The results demonstrate that the proposed RobotMover outperforms all baselines in both the simplified and full dynamic environments. The **RL** baseline exhibits the lowest average score with a high variance. This can be attributed to the lack of heuristic guidance, which causes the RL method to struggle in finding effective solutions and often leads to convergence at a suboptimal local minima. The **RL-EE** baseline improves upon RL by providing the global position of the end-effector, which corresponds to the robot-object contact position. In some chair and table experiments, **RL-EE** achieve similar results compared to **RobotMover**. However, since it lacks information about the robot’s arm pose, the robot often adopts unnatural arm configurations that are difficult to transfer to hardware. We will discuss this in the later section. The **RL-IK** baseline incorporates arm pose information by measuring the position of the end-effector in the robot’s local frame. While this approach provides localized guidance, it performs poorly in certain scenarios, such as when manipulating a chair (e.g., **RobotMover** achieves an 0.79 ± 0.04 score versus 0.55 ± 0.06 for **RL-IK**). This performance drop occurs because

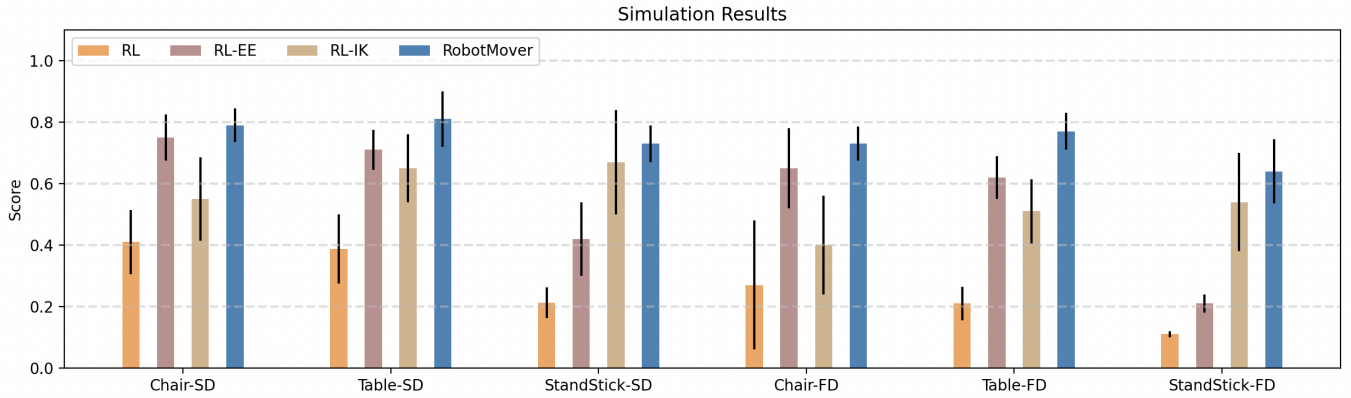


Fig. 6: Quantitative results of simulation experiments. Here, ‘SD’ represents simple-dynamics environment while ‘FD’ indicates full-dynamics environment. Our result indicates **RobotMover** outperform baseline methods in almost every settings.

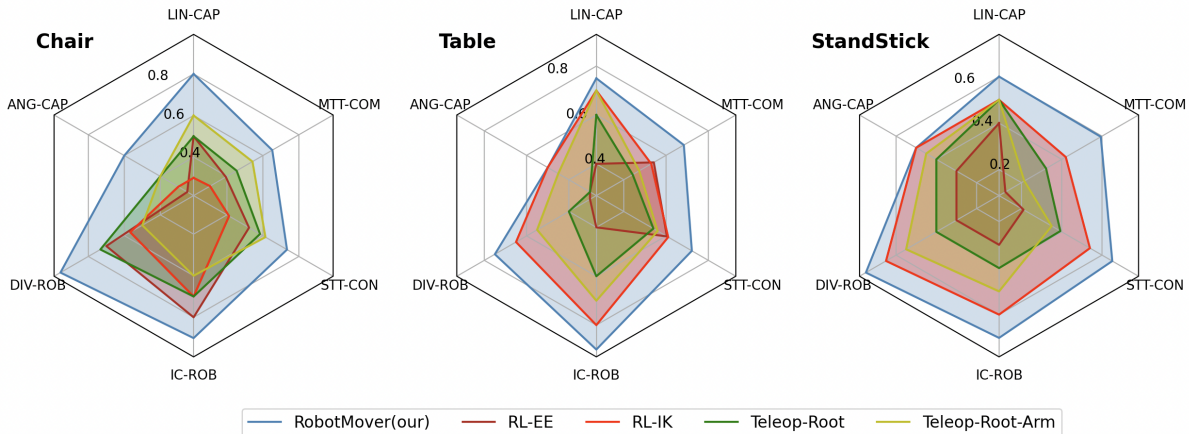


Fig. 7: Summary of Hardware Quantitative Results. We compare our proposed **RobotMover** with two learning-based baselines, **RL-EE** and **RL-IK**, as well as two teleoperation methods, **Teleop-Root** and **Teleop-Root-Arm**, across six evaluation metrics. The results show that **RobotMover** outperforms all baseline methods in every evaluation.

the arm poses measured in the robot’s local frame do not naturally translate into effective arm poses for the robot due to differences in morphology between humans and the robot, hence making the policy difficult to generalize to diverse target object velocity.

C. Hardware Experiments Setup

We conduct hardware experiments to evaluate the performance of our method in the real world. Experiments are performed using the Spot robot from Boston Dynamics. We deploy the policy trained in the simple dynamic simulation to the real-world robot without fine-tuning. To provide a comprehensive evaluation of our proposed method, we compare RobotMover against four baselines, including two learning-based methods and two teleoperation-based methods. These evaluations are conducted on three types of objects: chairs, tables, and racks, focusing on three aspects of the controller: capability, robustness, and controllability. In our hardware evaluation, unlike simulation where the robot is initialized at its default pose, we first teleoperate the robot to have a stable grasp with the target object and evaluate our method from that point, focusing on the performance of the ‘moving’ part.

The two learning-based baselines are **RL-EE**, **RL-IK** introduced in section: V-A. The two teleoperation baselines are:

- **Teleop-Root**: In this baseline, an operator teleoperates the robot by directly controlling its root linear and angular velocities, while the arm’s movements rely on the robot’s passive compliance for object interaction.
- **Teleop-Root-Arm**: Extending Teleop-Root, this baseline sets the robot arm’s desired position to the initial contact pose, providing a more direct arm control during manipulation.

The evaluation focuses on three critical properties of the controller, each capturing a unique dimension of performance. **Capability (CAP)** measures the robot’s ability to achieve maximum velocity while maintaining stability. **Robustness (ROB)** assesses the controller’s performance across varying conditions and object dynamics. **Controllability (CON)** evaluates the precision and accuracy of trajectory tracking during task execution.

We define two metrics for each of the properties in a total of six metrics:

- **Max Linear Velocity (LIN-CAP)**: Measures the maximum absolute linear velocity at which the robot can

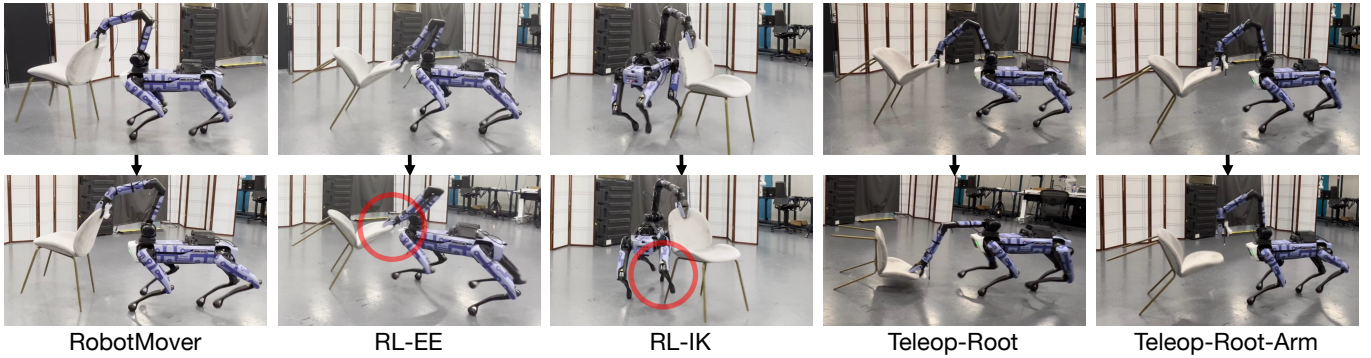


Fig. 8: Robot moving a chair using different methods. **RobotMover** shows stable chair moving. **RL-EE** and **RL-IK** result in robot self-collision and robot-object collision. **Teleop-Root** and **Teleop-Root-Arm** cannot stably move the chair, causing the chair to fall off.

operate stably without the object falling off the gripper or colliding with the robot. Stability is defined as maintaining control for 8 seconds. Each method is evaluated over 5 runs, with success requiring at least 4 successful trials. We measured the maximum linear velocity, starting at 0.5 m/s and adjusting by ± 0.05 m/s based on stability until the maximum was found.

- **Max Angular Velocity (ANG-CAP)**: Measures the maximum absolute angular velocity under the same stability criteria and measure strategy as LIN-CAP.
- **Object Diversity (DIV-ROB)**: Tests the trained policy on objects with varying weights and textures to assess robustness against different dynamics. For chairs, three variants with different textures and weights are used. For tables, two different tables are tested. For racks, a rack and a standing lamp are used for comparison. Success is measured by the robot moving these objects at medium speed for 8 seconds. For every object, we run 10 trials, and the score is measure by the success rate. $v^{DIV-ROB} = \frac{1}{10N} \sum_1^N \mathbf{1}(\text{if success})$. We list the objects we used for this experiment in the appendix.
- **Initial Condition Sensitivity (IC-ROB)**: Evaluates the sensitivity of the policy to variations in the initial contact condition. Small random perturbations are introduced, and the policy’s performance is assessed under these changes. In this experiment, we randomly sampled 3 initial contact poses close to the default contact pose. For each initial contact pose, we run 10 trials, and the score is also measure by the success rate. This leads to a total of $3 \times 10 = 30$ evaluations for a method on a single type of object.
- **Single Trajectory Tracking (STT-CON)**: Measures the endpoint difference between the robot’s planned rolling trajectory and the actual trajectory during single trajectory execution.
- **Multiple Trajectory Tracking (MTT-CON)**: Measures the endpoint difference for a sequence of trajectories generated by rolling out a series of planned trajectories. Compare to STT-CON, the metric measure also measure the motion transition property. The evaluation is the same

as we used in Section:V-A.

D. Hardware Comparison Results

We summarize our quantitative hardware evaluation in Figure 7. Overall, RobotMover outperforms all baselines over all metrics. For capability, RobotMover achieves the highest object-moving velocities, with a maximum linear velocity of 0.75 m/s and an angular velocity of 0.5 rad/s, while other methods struggle to maintain stability at such speeds, often resulting in the object falling off. In terms of robustness, our method demonstrates lower sensitivity to variations in object properties (e.g., weight, friction, thickness) and initial contact poses. Such variations introduce differences in inertia and contact forces, which can negatively impact policy performance. However, the learned RobotMover policy successfully handles to these dynamic changes, proving its potential for real-world application where the policy need to move diverse objects. In our experiment, RobotMoverpolicy is the only policy that able to move a large table and a heavy rack with success rate over 50%. For controllability, our result shows RobotMover achieves the best object velocity tracking performance over all types of objects. Other methods suffer either large sim2real gap or unsuitable root arm coordination which lead to inaccurate velocity tracking.

A qualitative comparison between RobotMover and learning-based methods is shown in Figure 8. Compared to the learning-based baselines (**RL-EE** and **RL-IK**), RobotMover leverages a dynamic chain representation, which leads to better task performance and facilitates sim-to-real transfer. Although **RL-EE** achieves good performance in simulation for chair and table manipulation, the learned policy’s desired arm pose on hardware often results in self-collisions, causing damage to the robot and leading to objects slipping off. Similarly, **RL-IK** exhibits poor hardware performance, as the policy frequently causes the object to collide with the robot’s rear legs, significantly degrading overall task execution as well as raising safety concerns to robot.

When compared to teleoperation methods, RobotMover also demonstrates clear advantages. Teleoperation heavily depends on the operator’s skill level, leading to lower capability and

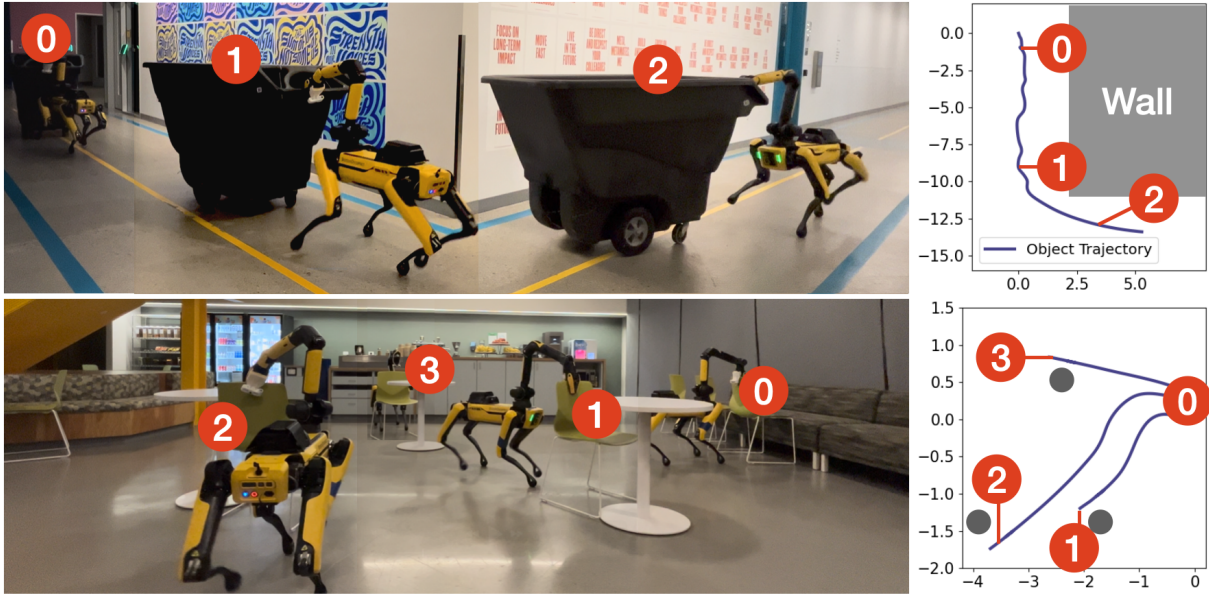


Fig. 9: Illustration of two applications: Trash Cart Transportation (top) and Chair Rearrangement (bottom). A motion planner determines the object trajectory for each task (right), our trained policy controls the robot to move the object of interest (left).

robustness under our experimental settings. Specifically, the RobotMover policy controls both the arm and root movements simultaneously while measuring the robot’s state at 20 Hz. This allows it to responsively adjust its actions to compensate for disturbances or oscillations—an ability that is nearly impossible for a human operator to achieve with the same level of precision. Additionally, in terms of controllability, teleoperation strategies primarily rely on root-level commands for the robot, whereas RobotMover’s policy operates in the object’s coordinate frame. This design enables RobotMover to achieve significantly better tracking performance. Figure 8 illustrates failure cases of the teleoperation methods. In particular, **Teleop-Root** fails to execute the appropriate torque, causing the chair to fall off. Moreover, **Teleop-Root-Arm** overemphasizes arm pose and root velocity, failing to maintain consistent movement of the chair.

E. Real World Applications

We demonstrate the capability of the learned policies to address complex real-world tasks by integrating them with high-level planners. Two applications are presented: *Trash Cart Transportation* and *Chair Rearrangement*. Trash cart transportation is a common task in office and residential environments where a loaded trash cart needs to be transported from one place to another. Chair rearrangement universally important task in various social and public settings, such as dining areas, meeting rooms, and event spaces. In our experiment, we integrate a learned object manipulation policy with a teleoperation-based high-level planner, we present interactive trash cart transportation. By integrating the policy with a heuristic object root velocity planner, we showcase automatic chair rearrangement. Snapshots illustrating these tasks are provided in Figure 9.

In the *Trash Cart Transportation* experiment, the robot’s

objective is to drag a large trash cart backward for approximately 10 meters along a hallway and then execute a 90-degree turn to transition to a perpendicular path. The trash cart, measuring approximately 1.8 m × 1.0 m × 1.2 m (L × W × H) and equipped with four wheels, is significantly larger than the robot itself. When manipulating the cart using the trained policy, the cart does not perfectly track the velocity command due to the asymmetrical weight distribution of the loaded cart and variations in contact status during the robot’s stepping motion.

To address this challenge, we employ an interactive control strategy. The user selects commands from a predefined set of temporary trajectories (a “cookbook”) using keyboard inputs. These commands dynamically guide the robot, ensuring the trash cart follows the desired path. Notably, the policy used in this experiment is the same policy trained for moving chairs, which are relatively lighter than the trash cart.

The results show that the large trash cart is successfully transported along the desired path. The trained policy adapts to the cart’s dynamics without fine-tuning. Notably, the robot’s root-arm coordination is evident during the object turning stage, where the robot follows a large arc while simultaneously adjusting the arm pose to guide the cart along a smaller arc. Our findings demonstrate that by combining the learned policy with an interactive control framework, the robot can reliably drag the trash cart along the specified route.

In the *Chair Rearrangement* experiment, the robot has to rearrange three chairs in a dining space of approximately 5 m × 4 m (L × W). The chairs are initially in the same location but each one has a different goal positions and orientations (headings) relative to the global frame. The goal positions and orientations are predetermined.

To achieve automatic chair rearrangement, we use a rule-based heuristic high-planner planner. This planner runs at

2Hz and commands target object velocities by comparing the object’s current global position and heading with the desired goal state. We describe the implementation of the heuristic planner in more detail in the Appendix. Spot’s onboard sensing system is utilized to determine the global positions of the robot and the chairs, while the end-effector position is used to approximate the objects’ positions. For simplicity, we assume that there are no obstacles between the starting positions and the target locations. Once a chair reaches its goal position, the robot is teleoperated to grasp and move the next chair.

Our results show that the robot can automatically place the chair in different goal states. On average, the robot takes approximately 30 seconds to move a chair 5 meters away while adjusting for a heading difference of $\pi/2$ radians. The system achieves an average tracking error of 0.15 meters in position and 0.3 radians in orientation. In addition, the chair used in this experiment has a different shape compared to the one used during training. Specifically, the experimental chair has a thinner back (4 mm in the experiment versus 10 mm in simulation), resulting in reduced contact force between the robot’s gripper and the chair. Lower contact force can potentially lead to reduced friction, increasing the likelihood of the chair slipping off the robot. However, the policy successfully adapts to this variation. We argue that this is due to the inclusion of friction randomization during training, enabling the policy to handle low-friction conditions effectively. These results highlight the system’s ability to perform precise and reliable chair rearrangement, underscoring the feasibility of automating such tasks in real-world environments.

F. Two-arm Demonstrations

Humans often use both arms to manipulate objects, but such demonstrations cannot be directly utilized to train a robot with only one arm, such as Spot. To address this challenge, we propose a simple solution: constructing a single dynamic chain by aggregating the dynamic chains of both arms and using the aggregated dynamic chain as a reference for training the robot policy. The aggregation is performed by selecting the midpoint between corresponding nodes on each chain to form the nodes of the aggregated chain:

$$x_t^{i,agg} = \frac{1}{2}(x_t^{i,l} + x_t^{i,r}). \quad (6)$$

Here, $x_t^{i,agg}$, $x_t^{i,l}$, and $x_t^{i,r}$ represent the positions of the i -th node on the aggregated dynamic chain, the left-arm dynamic chain, and the right-arm dynamic chain at time instance t , respectively. Once the positions of the aggregated nodes are obtained, the motion of the aggregated dynamic chain can be generated and used for training the robot policy. Notably, since both the left-arm and right-arm dynamic chains originate from the object’s root and terminate at the human root, the aggregated dynamic chain retains the same starting and ending nodes as the original chains.

We tested this method on a robot moving coffee tables using two-arm demonstrations. We separately evaluated the imitation performance on 10 demonstrations where the human

used a symmetric arm pose and 10 demonstrations where the human’s arms had different poses. The learning performance was assessed using the same object velocity tracking metric described in Section V-A.

For the symmetric pose experiment setting, the overall score reached 0.73 ± 0.10 , which is close to the single-arm demonstration result of 0.81 ± 0.09 . However, in the asymmetric setting, the overall score dropped to 0.35 ± 0.07 , which is even worse than the RL baseline score of 0.41 ± 0.11 . This result suggests that simply merging two asymmetric arm poses may not produce an effective reference dynamic chain. Averaging the positions of the two chains can lead to a reference chain that penetrates objects or exhibits other undesirable behaviors, ultimately degrading the training process.

VII. LIMITATIONS

Although our method achieves promising results, we recognize several limitations that we aim to address in the future.

The first limitation lies in our treatment of the object-grasping process. In this work, our focus is on how the robot dynamically manipulates the object after grasping, which led to less emphasis on the grasping phase itself. In simulation, we initialize the robot’s pose such that the gripper is close to the object, allowing it to make contact blindly. On hardware, the robot is manually initialized to grasp the object. Additionally, to ensure the control frequency as well as since the camera is blocked by the object after grasping, our control policy does not incorporate any camera input. In future work, we plan to develop a vision-based policy that enables the robot to navigate to the target object, grasp it at the correct contact location, to automatically provide initial contact conditions for the object moving policy.

Another limitation concerns the capability of the trained policies. While the proposed imitation method generalizes well to different objects and demonstrations, in this work, we train separate policies for different types of objects. Consequently, each policy is limited to handling objects with similar dynamic properties. In our future work, we aim to develop a single policy that can manage a wide variety of objects and execute diverse manipulation strategies, even for the same object. To achieve this, we intend to explore advanced techniques, such as diffusion policies, to enhance generalization and adaptability.

VIII. CONCLUSION

We introduce RobotMover, a framework to enable robots to move large objects in the real world by training them in simulation with human demonstrations. Critical to our method, is the Dynamic Chain, a novel graphical representation that enables to imitate human-object interactions in robot embodiments with different morphologies, facilitating the learning of reusable control policies. Our experimental evaluation in simulation demonstrates that policies trained using Dynamic Chain significantly outperform traditional robot learning methods in manipulating a variety of objects. Furthermore, our hardware experiments show that the proposed method produces more reliable object manipulation policies compared

to both learning-based approaches and teleoperation methods. Finally, we integrate the learned policies with various high-level planners, showcasing their applicability in diverse real-world daily tasks.

REFERENCES

- [1] Michael Ahn, Anthony Brohan, Noah Brown, Yevgen Chebotar, Omar Cortes, Byron David, Chelsea Finn, Chuyuan Fu, Keerthana Gopalakrishnan, Karol Hausman, et al. Do as i can, not as i say: Grounding language in robotic affordances. *arXiv preprint arXiv:2204.01691*, 2022.
- [2] Genesis Authors. Genesis: A universal and generative physics engine for robotics and beyond, December 2024. URL <https://github.com/Genesis-Embodied-AI/Genesis>.
- [3] Shikhar Bahl, Abhinav Gupta, and Deepak Pathak. Human-to-robot imitation in the wild. *RSS*, 2022.
- [4] Kevin Black, Noah Brown, Danny Driess, Adnan Esmail, Michael Equi, Chelsea Finn, Niccolo Fusai, Lachy Groom, Karol Hausman, Brian Ichter, et al. *pi_0*: A vision-language-action flow model for general robot control. *arXiv preprint arXiv:2410.24164*, 2024.
- [5] Anthony Brohan, Noah Brown, Justice Carbajal, Yevgen Chebotar, Joseph Dabis, Chelsea Finn, Keerthana Gopalakrishnan, Karol Hausman, Alex Herzog, Jasmine Hsu, et al. Rt-1: Robotics transformer for real-world control at scale. *arXiv preprint arXiv:2212.06817*, 2022.
- [6] Cheng Chi, Zhenjia Xu, Siyuan Feng, Eric Cousineau, Yilun Du, Benjamin Burchfiel, Russ Tedrake, and Shuran Song. Diffusion policy: Visuomotor policy learning via action diffusion. *The International Journal of Robotics Research*, page 02783649241273668, 2023.
- [7] Djork-Arné Clevert. Fast and accurate deep network learning by exponential linear units (elus). *arXiv preprint arXiv:1511.07289*, 2015.
- [8] Alejandro Escontrela, Xue Bin Peng, Wenhao Yu, Tingnan Zhang, Atil Iscen, Ken Goldberg, and Pieter Abbeel. Adversarial motion priors make good substitutes for complex reward functions. 2022 ieee. In *International Conference on Intelligent Robots and Systems (IROS)*, volume 2, 2022.
- [9] Zipeng Fu, Xuxin Cheng, and Deepak Pathak. Deep whole-body control: learning a unified policy for manipulation and locomotion. In *Conference on Robot Learning*, pages 138–149. PMLR, 2023.
- [10] Zipeng Fu, Tony Z Zhao, and Chelsea Finn. Mobile aloha: Learning bimanual mobile manipulation with low-cost whole-body teleoperation. *arXiv preprint arXiv:2401.02117*, 2024.
- [11] Caelan Reed Garrett, Rohan Chitnis, Rachel Holladay, Beomjoon Kim, Tom Silver, Leslie Pack Kaelbling, and Tomás Lozano-Pérez. Integrated task and motion planning. *Annual review of control, robotics, and autonomous systems*, 4(1):265–293, 2021.
- [12] Huy Ha, Yihuai Gao, Zipeng Fu, Jie Tan, and Shuran Song. Umi on legs: Making manipulation policies mobile with manipulation-centric whole-body controllers. *arXiv preprint arXiv:2407.10353*, 2024.
- [13] Noriaki Hirose, Dhruv Shah, Ajay Sridhar, and Sergey Levine. Exaug: Robot-conditioned navigation policies via geometric experience augmentation. In *2023 IEEE International Conference on Robotics and Automation (ICRA)*, pages 4077–4084. IEEE, 2023.
- [14] Edmond SL Ho, Taku Komura, and Chiew-Lan Tai. Spatial relationship preserving character motion adaptation. In *ACM SIGGRAPH 2010 papers*, pages 1–8. 2010.
- [15] Eric Jang, Alex Irpan, Mohi Khansari, Daniel Kappler, Frederik Ebert, Corey Lynch, Sergey Levine, and Chelsea Finn. Bc-z: Zero-shot task generalization with robotic imitation learning. In *Conference on Robot Learning*, pages 991–1002. PMLR, 2022.
- [16] Oussama Khatib, K Yokoi, K Chang, D Ruspini, R Holmberg, A Casal, and A Baader. Force strategies for cooperative tasks in multiple mobile manipulation systems. In *Robotics Research: The Seventh International Symposium*, pages 333–342. Springer, 1996.
- [17] Eric Krotkov, Douglas Hackett, Larry Jackel, Michael Perschbacher, James Pippine, Jesse Strauss, Gill Pratt, and Christopher Orłowski. The darpa robotics challenge finals: Results and perspectives. *The DARPA robotics challenge finals: Humanoid robots to the rescue*, pages 1–26, 2018.
- [18] Jiaman Li, Jiajun Wu, and C Karen Liu. Object motion guided human motion synthesis. *ACM Transactions on Graphics (TOG)*, 42(6):1–11, 2023.
- [19] Tianyu Li, Hartmut Geyer, Christopher G Atkeson, and Akshara Rai. Using deep reinforcement learning to learn high-level policies on the atrias biped. In *2019 International Conference on Robotics and Automation (ICRA)*, pages 263–269. IEEE, 2019.
- [20] Tianyu Li, Hyunyoung Jung, Matthew Gombolay, Yong Kwon Cho, and Sehoon Ha. Crossloco: Human motion driven control of legged robots via guided unsupervised reinforcement learning. *arXiv preprint arXiv:2309.17046*, 2023.
- [21] Tianyu Li, Jungdam Won, Alexander Clegg, Jeonghwan Kim, Akshara Rai, and Sehoon Ha. Ace: Adversarial correspondence embedding for cross morphology motion retargeting from human to nonhuman characters. In *SIGGRAPH Asia 2023 Conference Papers*, pages 1–11, 2023.
- [22] Chenhao Lu, Xuxin Cheng, Jialong Li, Shiqi Yang, Mazeyu Ji, Chengjing Yuan, Ge Yang, Sha Yi, and Xiaolong Wang. Mobile-television: Predictive motion priors for humanoid whole-body control. *arXiv preprint arXiv:2412.07773*, 2024.
- [23] Russell Mendonca, Emmanuel Panov, Bernadette Bucher, Jiuguang Wang, and Deepak Pathak. Continuously improving mobile manipulation with autonomous real-world rl. *arXiv preprint arXiv:2409.20568*, 2024.
- [24] Mayank Mittal, David Hoeller, Farbod Farshidian, Marco Hutter, and Animesh Garg. Articulated object interaction

- in unknown scenes with whole-body mobile manipulation. In *2022 IEEE/RSJ international conference on intelligent robots and systems (IROS)*, pages 1647–1654. IEEE, 2022.
- [25] Xue Bin Peng, Erwin Coumans, Tingnan Zhang, Tsang-Wei Edward Lee, Jie Tan, and Sergey Levine. Learning agile robotic locomotion skills by imitating animals. In *Robotics: Science and Systems*, 07 2020. doi: 10.15607/RSS.2020.XVI.064.
- [26] Yajvan Ravan, Zhutian Yang, Tao Chen, Tomás Lozano-Pérez, and Leslie Pack Kaelbling. Combining planning and diffusion for mobility with unknown dynamics. *arXiv preprint arXiv:2410.06911*, 2024.
- [27] Nikita Rudin, David Hoeller, Philipp Reist, and Marco Hutter. Learning to walk in minutes using massively parallel deep reinforcement learning. In *Conference on Robot Learning*, pages 91–100. PMLR, 2022.
- [28] Manolis Savva, Abhishek Kadian, Oleksandr Maksymets, Yili Zhao, Erik Wijmans, Bhavana Jain, Julian Straub, Jia Liu, Vladlen Koltun, Jitendra Malik, et al. Habitat: A platform for embodied ai research. In *Proceedings of the IEEE/CVF international conference on computer vision*, pages 9339–9347, 2019.
- [29] John Schulman, Filip Wolski, Prafulla Dhariwal, Alec Radford, and Oleg Klimov. Proximal policy optimization algorithms. *arXiv preprint arXiv:1707.06347*, 2017.
- [30] Nur Muhammad Shafiullah, Zichen Cui, Ariuntuya Arty Altanzaya, and Lerrel Pinto. Behavior transformers: Cloning k modes with one stone. *Advances in neural information processing systems*, 35:22955–22968, 2022.
- [31] Nur Muhammad Mahi Shafiullah, Anant Rai, Haritheja Etukuru, Yiqian Liu, Ishan Misra, Soumith Chintala, and Lerrel Pinto. On bringing robots home. *arXiv preprint arXiv:2311.16098*, 2023.
- [32] Sanjana Srivastava, Chengshu Li, Michael Lingelbach, Roberto Martín-Martín, Fei Xia, Kent Elliott Vainio, Zheng Lian, Cem Gokmen, Shyamal Buch, Karen Liu, et al. Behavior: Benchmark for everyday household activities in virtual, interactive, and ecological environments. In *Conference on robot learning*, pages 477–490. PMLR, 2022.
- [33] Charles Sun, Jędrzej Orbik, Coline Manon Devin, Brian H Yang, Abhishek Gupta, Glen Berseth, and Sergey Levine. Fully autonomous real-world reinforcement learning with applications to mobile manipulation. In *Conference on Robot Learning*, pages 308–319. PMLR, 2022.
- [34] Octo Model Team, Dibya Ghosh, Homer Walke, Karl Pertsch, Kevin Black, Oier Mees, Sudeep Dasari, Joey Hejna, Tobias Kreiman, Charles Xu, et al. Octo: An open-source generalist robot policy. *arXiv preprint arXiv:2405.12213*, 2024.
- [35] Jimmy Wu, Rika Antonova, Adam Kan, Marion Lepert, Andy Zeng, Shuran Song, Jeannette Bohg, Szymon Rusinkiewicz, and Thomas Funkhouser. Tidybot: Personalized robot assistance with large language models. *Autonomous Robots*, 47(8):1087–1102, 2023.
- [36] Keenan A Wyrobek, Eric H Berger, HF Machiel Van der Loos, and J Kenneth Salisbury. Towards a personal robotics development platform: Rationale and design of an intrinsically safe personal robot. In *2008 IEEE International Conference on Robotics and Automation*, pages 2165–2170. IEEE, 2008.
- [37] Haoyu Xiong, Russell Mendonca, Kenneth Shaw, and Deepak Pathak. Adaptive mobile manipulation for articulated objects in the open world. *arXiv preprint arXiv:2401.14403*, 2024.
- [38] Taozheng Yang, Ya Jing, Hongtao Wu, Jiafeng Xu, Kuankuan Sima, Guangzeng Chen, Qie Sima, and Tao Kong. Moma-force: Visual-force imitation for real-world mobile manipulation. In *2023 IEEE/RSJ International Conference on Intelligent Robots and Systems (IROS)*, pages 6847–6852. IEEE, 2023.
- [39] Sriram Yenamandra, Arun Ramachandran, Karmesh Yadav, Austin Wang, Mukul Khanna, Theophile Gervet, Tsung-Yen Yang, Vidhi Jain, Alexander William Clegg, John Turner, et al. Homerobot: Open-vocabulary mobile manipulation. *arXiv preprint arXiv:2306.11565*, 2023.
- [40] Naoki Yokoyama, Alex Clegg, Joanne Truong, Eric Undersander, Tsung-Yen Yang, Sergio Arnaud, Sehoon Ha, Dhruv Batra, and Akshara Rai. Asc: Adaptive skill coordination for robotic mobile manipulation. *IEEE Robotics and Automation Letters*, 9(1):779–786, 2023.
- [41] Yunbo Zhang, Deepak Gopinath, Yuting Ye, Jessica Hodgins, Greg Turk, and Jungdam Won. Simulation and retargeting of complex multi-character interactions. In *ACM SIGGRAPH 2023 Conference Proceedings*, pages 1–11, 2023.

A. Dataset Details

We selected human-object interaction demonstrations from the OMOMO dataset [18], a motion capture-based dataset featuring high-quality and diverse human and object movements. Although OMOMO contains demonstrations for more than ten objects, some, such as monitors, are not relevant to our task and were excluded. Additionally, objects that require significant two-arm manipulation, such as large boxes, were omitted to align with our study’s focus. Below, we summarize the number of demonstration trajectories used for training and their corresponding sources in the OMOMO dataset.

Object Type	Num	Demo Source
Chair	50	['woodchair', 'whitechair']
Table	50	['largetable', 'smalltable']
StandingStick	30	['floorlamp', 'clothesstand']

B. Diverse Objects Experiment

In Section VI-C, we introduce Object Diveristy(DIV-ROB) metrics to evaluate the robustness of the result policies by moving objects with different textures and weights. We summarize the objects for our diverse object test in Figure 10.



Name	Size(cm)	Note
Wood Chair	49*44*80	Medium Weight, Low Friction
Heavy Chair	55*52*80	Heavy, Medium Friction
Thin Chair	57*55*80	Medium Weight, Low Friction
Coffee Table	55*55*45	Medium Weight, Medium Friction
Heavy Table	57*144*42	Heavy, Low Friction
Standing Lamp	20*20*175	Light Weight, Low Friction
Standing Rack	60*60*175	Heavy, Low Friction

Fig. 10: The collection of objects used in the diverse object experiments.

C. Heuristic Planner for Chair Rearrangement

In the Chair Rearrangement experiment (Section VI-E), we use a heuristic planner for object target velocity planning. The planner first moves the object to the target location and then aligns its heading. The detailed planning policy is design as follows:

Algorithm 1 Heuristic Planner

Require: Target object position \bar{p}^{xy} and heading \bar{p}^{head} , position threshold $\bar{\delta}^{xy}$, heading threshold $\bar{\delta}^{yaw}$, robot policy π

```

1: // TARGET POSITION REACHING
2: repeat
3:   Measure the object position  $p^{xy}$  and the delta heading towards the
   target position  $\hat{p}^{head}$ .
4:   Target object velocity  $\bar{v}^o = [0.4, 0.0, \min(0.4, \hat{p}^{head})]$ .
5:   Run robot policy  $\pi$ .
6: until  $\|\bar{p}^{xy} - p^{xy}\| < \bar{\delta}^{xy}$ 

7: // TARGET HEADING ALIGNING
8: repeat
9:   Measure heading difference  $\delta^{head} = \bar{p}^{head} - p^{head}$ .
10:  Target object velocity  $\bar{v}^o = [0.0, 0.0, \min(0.4, \delta^{head})]$ .
11:  Run robot policy  $\pi$ .
12: until  $\|\delta^{head}\| < \bar{\delta}^{head}$ 

```

We found that this simple heuristic planner works well in our setting. However, for more complex tasks, such as those involving obstacle avoidance, a more sophisticated planner would be required.